JACS
JOURNAL OF THE AMERICAN CHEMICAL SOCIETY
Article
pubs.acs.org/JACS

Non-Fullerene Polymer Solar Cells Based on Alkylthio and Fluorine Substituted 2D-Conjugated Polymers Reach 9.5% Efficiency

Haijun Bin,[†,‡] Zhi-Guo Zhang,*[,†] Liang Gao,[†,‡] Shanshan Chen,[∥] Lian Zhong,[†] Lingwei Xue,[†] Changduk Yang,[∥] and Yongfang Li*[,†,‡,§]

[†]Beijing National Laboratory for Molecular Sciences, CAS Key Laboratory of Organic Solids, Institute of Chemistry, Chinese Academy of Sciences, Beijing 100190, China

[‡]University of Chinese Academy of Sciences, Beijing 100049, China

[§]Laboratory of Advanced Optoelectronic Materials, College of Chemistry, Chemical Engineering and Materials Science, Soochow University, Suzhou, Jiangsu 215123, China

[∥]Department of Energy Engineering, School of Energy and Chemical Engineering, Low Dimensional Carbon Materials Center, Ulsan National Institute of Science and Technology (UNIST), Ulsan 689-798, South Korea

Supporting Information

ABSTRACT: Non-fullerene polymer solar cells (PSCs) with solution-processable *n*-type organic semiconductor (*n*-OS) as acceptor have seen rapid progress recently owing to the synthesis of new low bandgap *n*-OS, such as ITIC. To further increase power conversion efficiency (PCE) of the devices, it is of a great challenge to develop suitable polymer donor material that matches well with the low bandgap *n*-OS acceptors thus providing complementary absorption and nanoscaled blend morphology, as well as suppressed recombination and minimized energy loss. To address this challenge, we synthesized three medium bandgap 2D-conjugated bithienyl-benzodithiophene-*alt*-fluorobenzotriazole copolymers **J52**, **J60**, and **J61** for the application as donor in the PSCs with low bandgap *n*-OS ITIC as acceptor. The three polymers were designed with branched alkyl (**J52**), branched alkylthio (**J60**), and linear alkylthio (**J61**) substituent on the thiophene conjugated side chain of the benzodithiophene (BDT) units for studying effect of the substituents on the photovoltaic performance of the polymers. The alkylthio side chain, red-shifted absorption down-shifted the highest occupied molecular orbital (HOMO) level and improved crystallinity of the 2D conjugated polymers. With linear alkylthio side chain, the tailored polymer **J61** exhibits an enhanced J_{SC} of 17.43 mA/cm^2, a high V_{OC} of 0.89 V, and a PCE of 9.53% in the best non-fullerene PSCs with the polymer as donor and ITIC as acceptor. To the best of our knowledge, the PCE of 9.53% is one of the highest values reported in literature to date for the non-fullerene PSCs. The results indicate that **J61** is a promising medium bandgap polymer donor in non-fullerene PSCs.

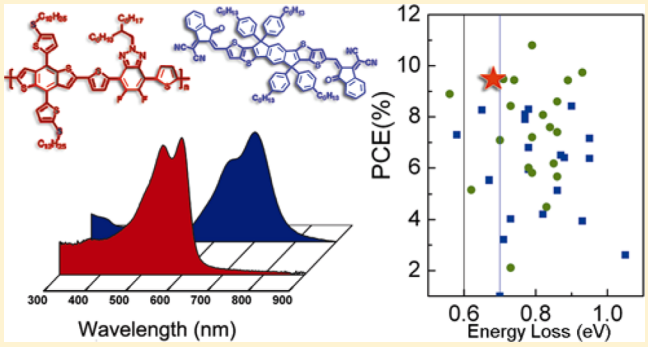

INTRODUCTION

Over the past decades, polymer solar cells (PSCs) with advantages of low-cost, light weight, and flexibility attracted extensive studies for the generation of affordable, clean, and renewable energy.[1] Generally, efficient PSCs adopt a bulk heterojunction structure, utilizing a *p*-type conjugated polymer as donor and an *n*-type material (fullerene derivatives, conjugated polymers, or organic semiconductors) as acceptor.[2] Currently, the most successful PSCs with power conversion efficiency (PCE) over 9% were achieved with fullerene derivatives as acceptor due to the special advantages of the fullerene acceptors such as high electron mobility, three-dimensional electron transfer, and transport, as well as formation of appropriate phase separation.[3−7] Despite the significant success of the fullerene derivative acceptors in PSCs, from both of application and scientific point of view, its intrinsic drawbacks, such as weak absorption of visible light, poor tunability of absorption and electronic energy levels, tedious purification, and high production costs, cannot be ignored.

In contrast to the widely studied fullerene acceptors, non-fullerene *n*-type organic semiconductor (*n*-OS) acceptors are emerging as an attractive competitive alternative due to their impressive advantages such as easy accessibility, strong absorption in the visible region, easily adjustable energy levels, and superior morphological stability in the blend film.[8] Encouraged by these advantages, a variety of D−A (donor−acceptor) structured *n*-OSs were specially designed and synthesized, with the electron-deficient (A) groups such as

Received: February 16, 2016
Published: March 21, 2016

DOI: 10.1021/jacs.6b01744
J. Am. Chem. Soc. 2016, 138, 4657−4664

Scheme 1. Synthesis Routes of Monomer M1 and the Polymers

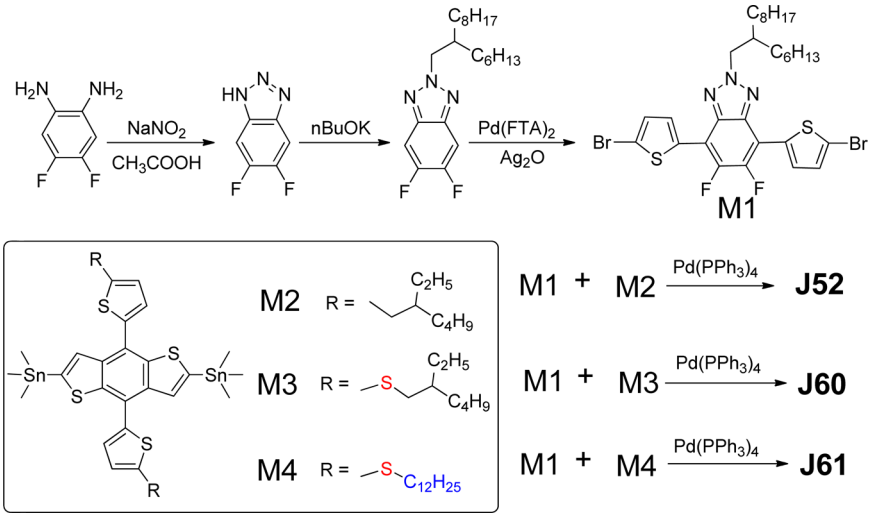

indanedione,[9] benzothiadiazole,[10] diketopyrolopyrrole,[11] and rylene dimide[12−22] etc. Also, different approaches including polymer donor selecting and morphological control, as well as interface engineering, are carried out for improving the photovoltaic performance of the non-fullerene PSCs.[11b,23,24] With these efforts, PCE of the non-fullerene PSCs has been steadily improved over 8%.[25−28]

Among the reported non-fullerene acceptors, low bandgap *n*-OS acceptors are more attractive to harvest light in the solar spectrum range. As a typical example, Zhan et al. recently reported an acceptor−donor−acceptor (A−D−A) structured low band gap *n*-OS acceptor ITIC[29] (as shown in Scheme 2) that exhibits good thermal stability and suitable energy levels, as well as relatively high electron mobility and strong absorption from 600 to 780 nm. Devices using low bandgap polymer PTB7-Th (with absorption band from 550 to 780 nm) as donor component achieved a primary PCE of 6.8%. Nevertheless, there is still some room for further improvement of the photovoltaic performance of the ITIC acceptor, because the IPCE values of the PSCs with PTB7-Th as donor in the wavelength region of 400−600 nm are low due to the weak absorption of both donor and acceptor components in the wavelength region. Obviously, the polymer donors with complementary absorption with ITIC acceptor could further improve the photovoltaic performance of ITIC.

In addition to the absorption issue, it is also very important for the polymer donor to appropriately aggregate and to form nanoscaled donor/acceptor interpenetrating network in the blend active layer of the non-fullerene PSCs. For the traditional fullerene acceptor, its spherical molecular structure, isotropic electron-transporting property, and self-aggregation characteristic make it compatible with a large number of donor materials. Whereas for the *n*-OS acceptors such as ITIC, its planar molecular structure makes its aggregation behavior different from that of fullerene acceptors. Therefore, matching with the *n*-OS acceptor in the morphology and charge-transporting issue should also be considered in selecting polymer donors in the non-fullerene PSCs. Actually, two-dimension (2D)-conjugated polymers with conjugated side chains have shown better photovoltaic performance in comparison with the polymers without the conjugated side chains in the non-fullerene PSCs,[30] which may be ascribed to the better matching of the 2D polymer donor with the *n*-OS acceptor in the aspects of morphology and charge transportation.

Very recently, we utilized a 2D-conjugated polymer J51 with medium bandgap (1.91 eV) as donor in the all polymer PSCs with nanphthalene diimide-*alt*-bithiophene (N2200) as polymer acceptor and realized a high PCE of 8.27% together with a high fill factor of 70.24%.[28] The high efficiency is benefitted from the deeper HOMO level and higher hole mobility of J51, which is a 2D-conjugated D−A copolymer of bithienyl-benzodithiophene (BDTT) and fluorine substituted benzotriazole (FTAZ), and complementary absorption of J51 with N2200. Encouraged by the success of the polymer J51, herein, we performed systematic side chain engineering on the 2D-conjugated bithienyl-benzodithiophene (BDTT)-*alt*-fluorobenzotriazole D−A copolymers, and used the polymers as donor in the non-fullerene PSCs with ITIC as acceptor. Three D−A copolymers were synthesized based on fluorobenzotriazole with branched alkyl substituent as acceptor (A) unit and BDTT with branched alkyl (**J52**), branched alkylthio (**J60**), and linear alkylthio (**J61**) substituent on thiophene conjugated side chains as donor (D) unit. The incorporation of the alkylthio substitution is inspired by its special-function in forming p_π(C)−d_π(S) orbital overlap between the conjugated side chains and the alkylthio substitution, thus down-shifting the highest occupied molecular orbital (HOMO) levels and red-shifting absorption.[31] The design of the substituent structures on BDTT unit in the three polymers is for the studies of the effect of alkylthio side chain and the side chain conformation on the photovoltaic performance of the polymers, as side chain effect is an important issue in conjugated polymers that determine their physicochemical properties.[30d,32] Among the three polymers, **J61** with linear alkylthio side chain exhibits a maximum PCE of 9.53% with an enhanced J_{SC} of 17.43 mA/cm^2 and a high V_{OC} of 0.89 V in the ITIC-based non-fullerene PSCs. To the best of our knowledge, the PCE of 9.53% is one of the highest values reported in literature to date for non-fullerene PSCs. The results indicate that **J61** is a promising medium bandgap polymer donor material for non-fullerene PSCs.

RESULTS AND DISCUSSION

Materials Synthesis. The synthetic routes of monomer M1 and the copolymers are depicted in Scheme 1 and the chemical

DOI: 10.1021/jacs.6b01744
J. Am. Chem. Soc. 2016, 138, 4657−4664

structures of the polymer donors and ITIC acceptor are shown in Scheme 2. The monomers and copolymers were synthesized

Scheme 2. Chemical Structures of the Copolymers and Low Bandgap *n*-OS acceptor ITIC

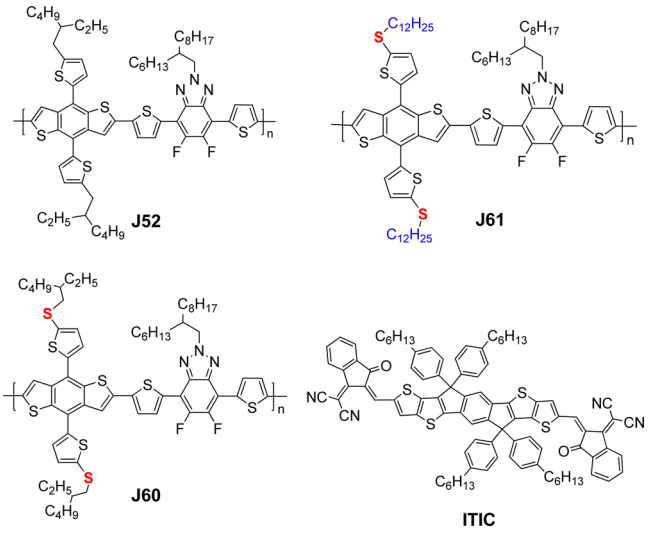

according to the procedure in our previous publication[31a,33] and related references.[34] For ensuring the polymers solubility, we introduced a bulky branched 2-hexyldecyl side chain in monomer M1, whereas for the investigation of side chain effect on the photovoltaic performance of the polymers, we designed different side chains on BDTT unit: 2-ethylhexyl group in M2, 2-ethylhexylthio group in M3, and dodecylthio group in M4. The polymers were synthesized by the palladium-catalyzed Stille-coupling polymerization with high yield.[35] Molecular weights of the polymers were measured by gel permeation chromatography (GPC), as listed in Table 1. The number-average molecular weights (M_n) of **J52**, **J60**, and **J61** are 57.5, 23.9, and 32.4 KDa with corresponding polydispersity index (PDI) of 1.86, 2.22, and 2.29, respectively. The polymers can be readily dissolved in common organic solvents, such as chloroform, 1-chlorobenzene, and 1,2-dichlorobenzene at room temperature.

Thermogravimetric analysis (TGA) was carried out to evaluate the thermal stability of the polymers. The TGA plots of the polymers are shown in Figure S1 in Supporting Information (SI), and their thermal decomposition temperatures (T_d) at 5% weight loss were also listed in Table 1. The T_d values of **J52**, **J60**, and **J61** are 312, 295, and 345 °C, respectively, which indicate that the thermal stability of the polymers is high enough for their application in PSCs.

Absorption Spectra and Electronic Energy Levels of the Polymers. Figure 1a shows the absorption spectra of the polymers and ITIC (for comparison) films. All the three polymers have well-defined absorption peaks with vibronic shoulder in the longer wavelength range which indicates the existence of ordered aggregation and strong $\pi-\pi$ stacking interaction in the polymer films. **J52** film shows two absorption peaks at 538 and 590 nm, respectively, with absorption edge at 630 nm, corresponding to an optical bandgap of 1.96 eV, while the absorption spectra of **J60** and **J61** films display the same absorption edges at 642 nm (corresponding to an optical bandgap of 1.93 eV) which is red-shifted by ca. 10 nm in comparison to that of **J52** film. The red shift of the absorption of the **J60** and **J61** films should result from the alkylthio substituent of the two polymers. Obviously, all the three polymers demonstrated complementary absorption with that of **ITIC** acceptor in the vis-NIR region, as shown in Figure 1a. The film maximum extinction coefficients of the copolymers are high: 7.3×10^4 cm^{-1} for **J52**, 6.6×10^4 cm^{-1} for **J60**, and 8.6×10^4 cm^{-1} for **J61**. The absorption spectra of the blend films of polymer/ITIC, as shown in Figure S2 in SI, cover a broad wavelength range from 400 to 780 nm, which further confirms the well matched complementary absorption of the polymer donor and the ITIC acceptor.

As we know, energy level matching of donor and acceptor materials is an important factor to achieve high-performance PSCs. Cyclic voltammetry (CV) was employed to evaluate HOMO energy level (E_{HOMO}) and LUMO energy level (E_{LUMO}) of the polymers. The onset oxidation/reduction potentials (E_{ox}/E_{red}) of the polymers, as shown in Figure 1b, are 0.81/−1.41 V vs. Ag/AgCl for the alkyl chain substituted **J52**. The E_{HOMO} and E_{LUMO} levels of **J52** were calculated to be −5.21 and −2.99 eV, respectively, according to the equations: $E_{HOMO/LUMO} = -e\,(E_{ox/red} + 4.40)$ (eV). For **J60** and **J61** with alkylthio substitution, their E_{HOMO} and E_{LUMO} levels are down-shifted to −5.32 and −3.08 eV, respectively. The E_{HOMO} of **J60** and **J61** is 0.11 eV deeper than that of **J52**, which will benefit for higher V_{oc} of the PSCs with the polymers as donor. For **ITIC** acceptor, E_{HOMO} and E_{LUMO} are located at −5.48 and −3.83 eV, respectively.[29] Notably, the HOMO energy offset (ΔE_{HOMO}) between **J60** or **J61** and **ITIC** is only 0.16 eV, which is smaller than the empirical threshold of 0.3 eV for effective exciton dissociation to overcome the binding energy of the excitons. Interestingly, hole transfer from **ITIC** to **J60** or **J61** appears to be highly efficient, as can be seen from the photoluminescence (PL) quenching experiments and the high photo response in the range of 650−800 nm, as discussed in more details below.

Photovoltaic Properties. Polymer solar cells were fabricated with a conventional device structure of ITO (indium tin oxide)/PEDOT:PSS (poly(3,4-ethylenedioxythiophene):poly(styrene-sulfonate))/polymer donor:**ITIC** (1:1, w/w)/PDINO (perylene diimide functionalized

Table 1. Molecular Weights, Thermal and Physicochemical Properties of the Copolymers

copolymers	M_n (g mol^{-1})	PDI (M_w/M_n)	T_d (°C)[a]	λ_{max} (nm)[b]	λ_{edge} (nm)[c]	E_g^{opt} (eV)[d]	E_{HOMO} (eV)[e]	E_{LUMO} (eV)[e]	E_g^{ec} (eV)[f]
J52	57.5K	1.86	312	538, 590	630	1.96	−5.21	−2.99	2.22
J60	23.9K	2.22	295	550, 598	642	1.93	−5.32	−3.08	2.24
J61	34.2K	2.29	345	552, 600	642	1.93	−5.32	−3.08	2.24

[a]5% weight-loss temperature measured by TGA under nitrogen. [b]Polymer films on quartz plate cast from chloroform solution. [c]Absorption edge of the polymer films. [d]Calculated from the absorption edge of the polymer films: $E_g^{opt} = 1240/\lambda_{edge}$. [e]Calculated according to the equation: $E_{HOMO/LUMO} = -e(E_{ox/red} + 4.40)$ (eV). [f]Electrochemical bandgap obtained from $E_{LUMO} - E_{HOMO}$.

DOI: 10.1021/jacs.6b01744
J. Am. Chem. Soc. 2016, 138, 4657−4664

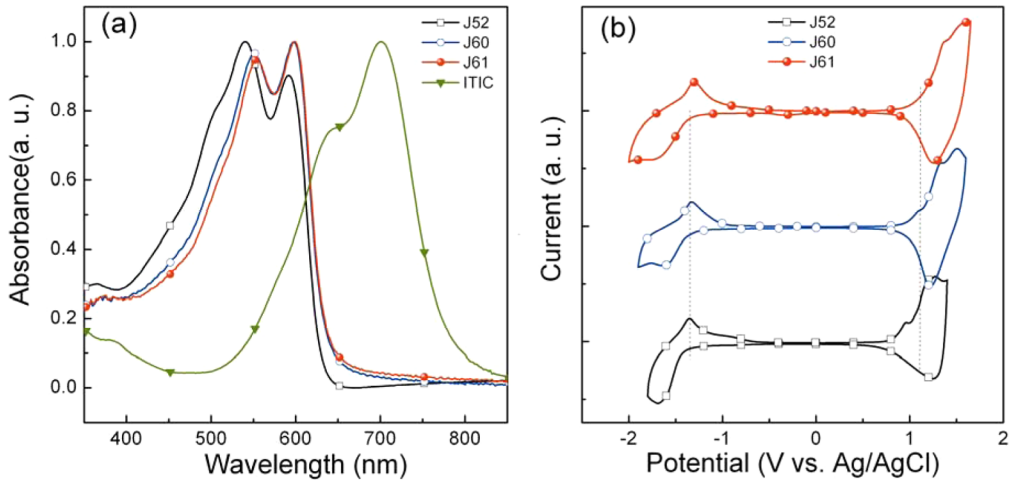

Figure 1. (a) Absorption spectra of the polymers and ITIC in film states. (b) Cyclic voltammograms of the polymers.

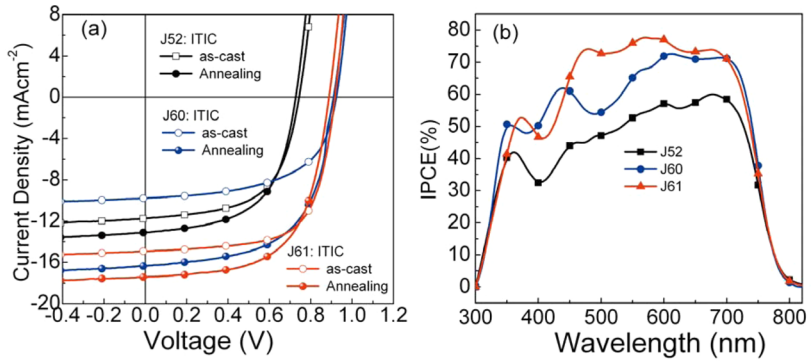

Figure 2. (a) Typical $J-V$ characteristics of the PSCs based on polymer donor/ITIC (1:1, w/w) with (annealing) or without (as-cast) thermal annealing at 100 °C for 10 min, under the illumination of AM1.5G, 100 mW/cm^2. (b) The IPCE spectra of the PSCs with thermal annealing at 100 °C for 10 min.

Table 2. Photovoltaic Performance Parameters of the PSCs Based on Polymer/ITIC (1:1, w/w), under the Illumination of AM1.5G, 100 mW/cm^2

devices	V_{oc}[c] (V)	J_{sc}[c] (mA/cm^2)	FF[c] (%)	PCE[c] (%)	R_s[d] Ω·cm^2	R_p[e] kΩ·cm^2	μ_h 10^{-4} cm^2 v^{-1} s^{-1}	μ_e 10^{-4} cm^2 v^{-1} s^{-1}
J52/ITIC[a]	0.74	11.73	59.36	5.18	12.26	0.68	1.01	0.31
	(0.74 ± 0.001)	(11.30 ± 0.51)	(58.24 ± 1.44)	(4.85 ± 0.26)				
J52/ITIC[b]	0.73	13.11	57.80	5.51	11.59	0.57	1.22	0.35
	(0.73 ± 0.001)	(12.45 ± 0.56)	(58.10 ± 0.56)	(5.26 ± 0.18)				
J60/ITIC[a]	0.92	9.78	57.45	5.17	15.04	0.95	0.75	0.21
	(0.92 ± 0.001)	(9.32 ± 0.46)	(59.02 ± 1.56)	(5.07 ± 0.14)				
J60/ITIC[b]	0.91	16.33	60.38	8.97	8.62	0.65	1.99	1.46
	(0.91 ± 0.001)	(15.84 ± 0.49)	(59.79 ± 2.03)	(8.67 ± 0.31)				
J61/ITIC[a]	0.91	14.95	66.55	9.15	9.24	0.96	1.59	1.45
	(0.91 ± 0.001)	(15.09 ± 0.36)	(64.75 ± 1.81)	(8.93 ± 0.26)				
J61/ITIC[b]	0.89	17.43	61.48	9.53	9.34	1.01	4.96	2.16
	(0.89 ± 0.001)	(17.02 ± 0.38)	(61.08 ± 0.74)	(9.22 ± 0.24)				

[a]As-cast film. [b]With thermal annealing at 100 °C for 10 min. [c]The values in parentheses are average values obtained from 10 devices. [d]Calculated from the inverse slope at $V = V_{oc}$ in $J-V$ curves under illumination; [e]Calculated from the inverse slope at $V = 0$ in $J-V$ curves under illumination.

with amino *N*-oxide)/Al, where PDINO was selected as the cathode buffer layer because of its high performance in PSCs.[36] Figure 2 shows the current density–voltage ($J-V$) curves, and the corresponding incident photon to converted current efficiency (IPCE) spectra of the optimized devices, and the photovoltaic performance data were listed in Table 2 for a clear comparison. The active layers of the optimized devices were spin-coated from their chloroform solution with a donor/acceptor (D/A) weight ratio of 1:1 followed by thermal annealing at 100 °C for 10 min. For comparison, devices without the thermal annealing treatment were also fabricated.

The PSC based on **J52/ITIC** (1:1, w/w) without thermal annealing delivers a PCE of 5.18% with a V_{OC} of 0.74 V, J_{sc} of 11.73 mA/cm^2, and FF of 59.36%. For the alkylthio substituted

DOI: 10.1021/jacs.6b01744
J. Am. Chem. Soc. 2016, 138, 4657–4664

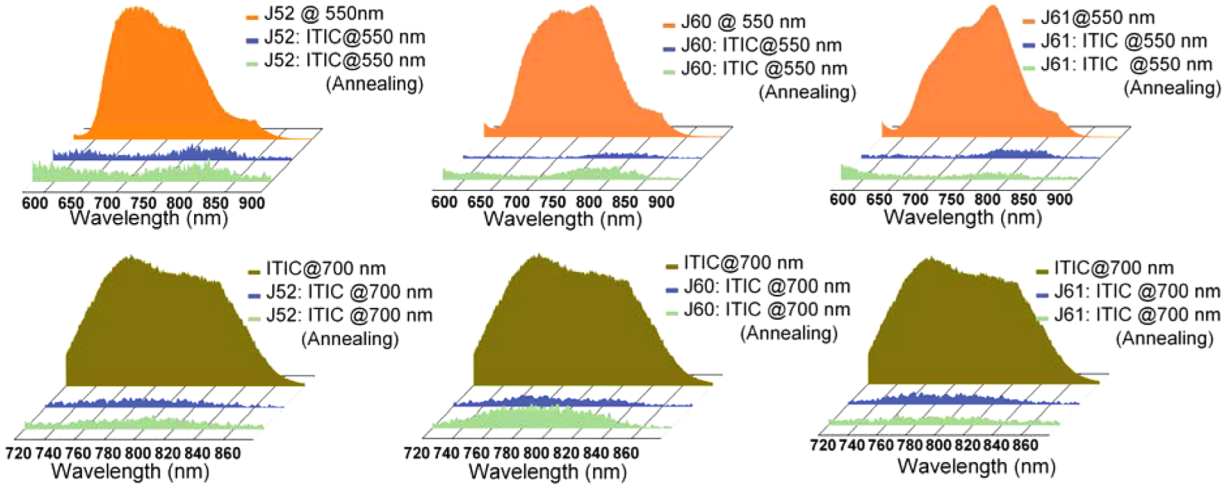

Figure 3. Photoluminescence spectra of pure **J52**, **J60**, **J61** (excited at 550 nm) and **ITIC** (excited at 700 nm) as well as the blend films of **J52**/**ITIC**, **J60**/**ITIC**, and **J61**/**ITIC** (excited at 550 and 700 nm) with and without thermal annealing.

J60 and **J61** based devices, one obviously advantage is their high V_{OC} values of ca. 0.90 V due to their low E_{HOMO} values, indicating the success of our molecular design in lowering the HOMO level by side chain engineering of alkylthio substitution. For the two alkylthio substituted polymers, even without any device treatment, **J61** demonstrated significantly high PCE of 9.15% with a J_{SC} of 14.95 mA/cm^2, whereas for **J60**, PCE of 5.17% with a lower J_{SC} of 9.78 mA/cm^2 was only obtained. For the three polymers, the thermal annealing at 100 °C for 10 min dramatically improved the device performance. The PCE values of the best PSCs based on **J52**, **J60**, and **J61** increased to 5.51%, 8.97%, and 9.53%, respectively. To the best of our knowledge, the PCE values of the **J60**- and **J61**-based devices are at the top of non-fullerene PSCs reported in the literatures to date, especially the PCE of 9.53% for the PSC based on **J61** is one of the highest efficiency for the non-fullerene PSCs.

One dramatic effect of the thermal annealing is the increase of J_{SC} values, as can be seen from Table 2 and Figure 2. After the thermal annealing, their J_{SC} values are increased from 11.73 to 13.11 mA/cm^2 for **J52**-based PSC, from 9.78 to 16.33 mA/cm^2 for **J60**-based PSC, and from 14.95 to 17.43 mA/cm^2 for **J61**-based PSC.

The high J_{SC} values of the devices with thermal annealing can be confirmed from their IPCE spectra (Figure 2b). Along with the broad photo response from 300 to 800 nm, the maximum values reached 60%, 72%, and 78% for the PSCs based on **J52**, **J60**, and **J61**, respectively, indicating efficient photon harvesting and charge collection in the active layers. For the PSC based on **J61**/**ITIC**, its high IPCE values in the range of 650−800 nm illustrates that efficient hole transfer from **ITIC** to **J61** did happen although the E_{HOMO} difference between **J61** and **ITIC** is only 0.16 eV. The result indicates that the exciton binding energy of ITIC *n*-OS could be quite low, at least lower than 0.16 eV, which is very important for high performance organic semiconductor photovoltaic materials. The J_{SC} values calculated from the IPCE spectra were 12.48, 15.56, and 16.67 mA/cm^2 for the devices based on **J52**, **J60**, and **J61**, respectively, which are in good agreement with the J_{SC} values obtained from the *J*−*V* curves within a 5% mismatch.

To further understand the thermal annealing effect on the device performance, the bulk charge transport properties of the polymer/ITIC blends were investigated using the space charge-limited current (SCLC) method with the hole only device (ITO/PEDOT:PSS/active layer/Au) and electron only device (ITO/ZnO/active layer/PDINO/Al). The plots of the current density vs voltage for the devices are shown in Figure S3 in SI. The hole (μ_h)/electron (μ_e) mobilities of the **J61**/**ITIC** film are calculated to be 1.59×10^{-4} cm^2 v^{-1} s^{-1}/1.45×10^{-4} cm^2 v^{-1} s^{-1} for the as-cast film and 4.96×10^{-4} cm^2 v^{-1} s^{-1}/2.16×10^{-4} cm^2 v^{-1} s^{-1} for the annealed film. Apparently, after thermal annealing, charge carrier mobilities were increased for some extent. Similar trends were also observed in the blend films of **J60**:**ITIC**, and **J52**:**ITIC**. The results suggest that the increased charge carrier mobilities after thermal annealing are beneficial to the improvement of the device performance. In comparison with the charge carrier mobilities of the annealed devices, it can be found that the devices based on the alkylthio substituted copolymers (**J60** and **J61**) demonstrated high and balanced hole and electron mobilities, which should be one reason for their higher J_{SC} and high PCE values.

It should be mentioned that You et al. effectively enhanced the hole mobility of conjugated D−A copolymers of benzodithiophene (BDT) and benzotriazole (TAZ) by fluorine substitution on TAZ unit.[34b] Our results confirm the positive effect of the fluorine substitution of TAZ unit on hole mobility of the corresponding D−A copolymers. In addition to the influence of the fluorine substitution, our results also indicate that the side chain engineering, such as the alkylthio substitution on thiophene conjugated side chain of BDT unit, is another effective way to improve the hole mobility of the D−A copolymers based on BDT and TAZ.

Photoluminescence (PL) quenching experiment was carried out to confirm the above-mentioned exciton dissociation and charge transfer behavior in the blends, where excitation wavelengths of 500 nm for polymer donors and 700 nm for **ITIC** were selected according to their maximum absorptions. Figure 3 shows the PL spectra of the blend films in comparison with those of pure polymer or **ITIC** films. When excited at a wavelength of 500 nm, PL emission peak of the polymer donors appears in the range of 600−850 nm centered at 680 nm. For the blend films, their emissions were almost all quenched (by over 95%), suggesting effective electron transfer from the polymers to **ITIC** for the excitons generated in the donor phase. For the **ITIC** acceptor, its emission was found in the range of 800−900 nm when excited at a wavelength of 700

DOI: 10.1021/jacs.6b01744
J. Am. Chem. Soc. 2016, 138, 4657−4664

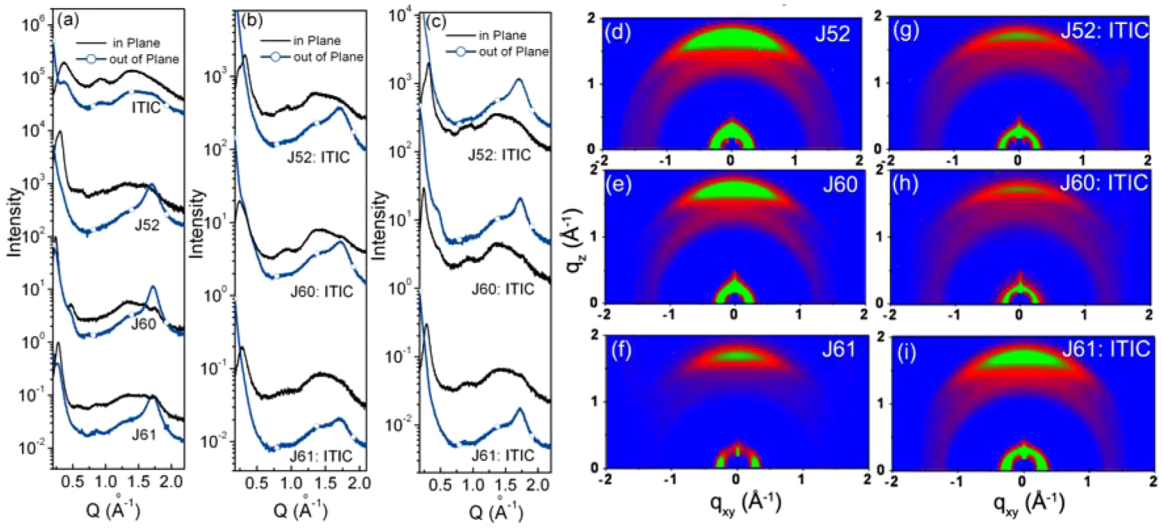

Figure 4. Line cuts of the GIWAXS images of (a) pristine polymer films and ITIC film, (b) as cast polymer/ITIC blend films and (c) thermal annealed polymer/ITIC blend films. (d–f) GIWAXS images of the pristine polymer films and (g–i) GIWAXS images of thermal annealed polymer/ITIC blend films. The sample names are labeled on the figures.

nm. For the blend films, the PL spectra were effectively quenched (by 93% for **J60** and 96% for **J52** and **J61**) when using the photo excitation at 700 nm. For the excitons generated in the acceptor phase, this quenching experiment means effective hole transfer from **ITIC** acceptor to polymer donor, which further confirm the efficient charge transfer between the ITIC acceptor and the polymer donor under such a small E_{HOMO} difference of 0.16 eV.

Morphological Characterization. To explain the good photovoltaic performance of the non-fullerene PSCs, we measured the microstructure and surface morphologies of the polymer films and the blend films by grazing incident wide-angle X-ray diffraction (GIWAXS) plots[37] and tapping-mode atomic force microscopy (AFM). Figure 4 and Figure S4 in SI show the plots and images of the GIWAXS measurements, and Table S1 in SI lists the structure parameters of the polymers in the pure polymer and in the blend films obtained from the GIWAXS measurements. Strong diffraction peaks of the pure polymer films, as shown in Figure 4a, reveal the semicrystalline structure and strong preference for face-on orientation in the polymer films. With the substituents changed from alkyl (**J52**) to branched alkylthio (**J60**) and then to linear alkylthio (**J61**), the lamellar distances as revealed by the (100) peaks are gradually increased from **J52** to **J61**: 21.11 Å for **J52**, 22.48 Å for **J60**, and 26.11 Å for **J61** (see Table S1 in SI). Clearly, the lamellar distances are affected by the length of the substituents, whereas for the facial $\pi-\pi$-stacking distances as revealed by the (010) peaks, an opposite trend was observed: 3.70 Å for **J52**, 3.67 Å for **J60**, and 3.65 Å for **J61** (see Table S1 in SI). The results suggest both the type and topology of the substituents affect the aggregation state: the alkylthio substituent promotes the $\pi-\pi$ stacking interaction and most specially linear alkylthio chains may reduce steric hindrance more than branched alkylthio chains in an aggregation state thus demonstrating tightest $\pi-\pi$ stacking in this series of polymers.[15] The lamellar (100) peak of **ITIC** is located at 0.318 Å $^{-1}$ with lamellar distance of 16.67 Å. The weakness of (010) $\pi-\pi$ stacking peak for **ITIC** film is due to the steric effect of tetrahexylphenyl substituents, which prevents $\pi-\pi$ stacking of the **ITIC** molecules.

For the polymer blend films, the GIWAXS plots (Figure 4b) show semicrystalline structure with the diffraction patterns as the summation of diffraction patterns from individual components, indicating that the polymers in the blend are crystallizing in a similar manner as that in its pure polymer film. After thermal annealing treatment, the blend films show predominant face-on orientation (Figure 4c). Further looking into the donor component, it can be found that, significantly stronger peak intensity along with narrower (010) peak width of polymer components were observed for all the samples (Figure 4 and Table S1). Notably, the facial $\pi-\pi$-stacking distances are decreased. All these characteristics are associated with its higher crystalline behavior of the blend film, and the strong face-on orientation and the shorter $\pi-\pi$-stacking distances are desirable for higher charge carrier mobility thereby higher photovoltaic efficiencies, as discussed above.

The AFM images, as shown in Figure S5 in SI, reveal that the blend films have relatively smooth surface with a root-mean-square (RMS) roughness of 0.70 nm for **J60**/**ITIC** blend film and 0.50 nm for **J61**/**ITIC** blend film, while relatively coarse surface with RMS roughness of 0.837 nm for **J52**/**ITIC** blend film, suggesting that the alkylthio substituted polymers can provide better miscibility with **ITIC** in the blend films. The AFM phase images (Figure S5 in SI) of the blend films reveal evidence of a large domains of 30–40 nm for the **J52**/**ITIC** blend film and a well-distributed nanofibrillar networks around 10–20 nm for the **J60**/**ITIC** and **J61**/**ITIC** blend films. Notably, the **J61**/**ITIC** blend film shows more preferred domain size of ∼10–15 nm, which certainly accounts for its observed superior device performance.

Energy Loss. A challenge facing the studies of PSCs is how to manage the electronic energy levels of the polymer donor and acceptor (fullerene or non-fullerene) components in the blend active layers to simultaneously maximize the V_{OC} and the J_{SC} for higher PCE. However, it is a well-known fact that there is a trade-off between V_{OC} and J_{SC}. A crucial issue in pursuing higher PCE is to minimize the energy loss (E_{loss}) of the PSCs. E_{loss} is defined as $E_{loss} = E_g - eV_{OC}$, where E_g is the lowest optical band gap of the donor and acceptor components.[38] The reported E_{loss} in the literatures is typically 0.7–1.0 eV.[38c] Figure

DOI: 10.1021/jacs.6b01744
J. Am. Chem. Soc. 2016, 138, 4657–4664

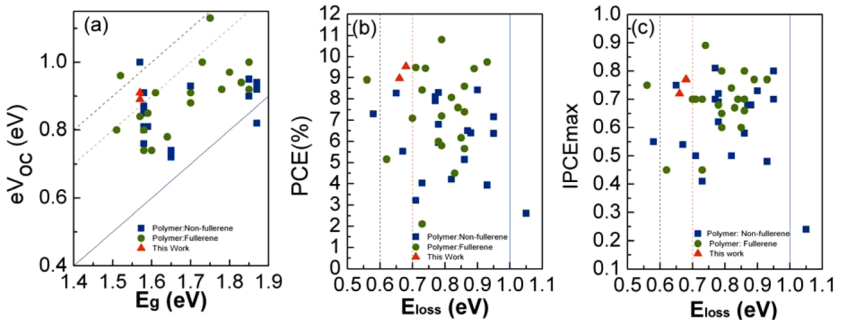

Figure 5. (a) Plots of eV_{OC} against E_g as well as (b) PCE and (c) IPCE_{max} against E_{loss} in various PSCs with fullerene or non-fullerene acceptors. The black dotted lines are the lines of E_{loss} = 0.6 eV, the red dotted lines, E_{loss} = 0.7 eV, and the blue lines, E_{loss} = 1.0 eV.

5a shows the plots of eV_{OC} against E_g in this work in comparison with various PSC devices (see Table S2 in SI) for the photovoltaic performance data points (shown in Figure 5) reported in literatures. The optical band gap of **ITIC** film estimated from its absorption edge (788 nm) is 1.57 eV. For the PSCs with **ITIC** as acceptor, the V_{OC} of the PSC based on **J52** is 0.74−0.73 V (see Table 2), thus E_{loss} in this device is 0.83−0.84 eV, which is among the typical E_{loss} values for the PSCs. while the V_{OC} values of the PSCs based on **J60** and **J61** with alkylthio substituent are 0.89−0.92 V so that the E_{loss} in the devices is 0.68−0.65 eV, which is smaller than that of most PSCs and approaching the empirically low threshold of 0.6 eV.[38a] The plots of PCE and the maximum IPCE (IPCE_{max}) against E_{loss} are provided in Figure 5, panels b and c, respectively. It is noted that PCE and the IPCE_{max} (78.0%) of the PSC based on **J61**/**ITIC** are in fact the highest values among the fullerene and non-fullerene PSCs having E_{loss} less than 0.7 eV. Such small E_{loss} along with high PCE and IPCE_{max} are benefitted from the very small ΔE_{HOMO} of 0.16 eV in the PSCs based on **J61**/**ITIC**.

CONCLUSION

Three medium bandgap and 2D-conjugated bithienyl-benzodithiophene-*alt*-fluorobenzotriazole copolymers **J52**, **J60**, and **J61** with alkyl or alkylthio substituents on thiophene conjugated side chains were designed and synthesized for the application as donor materials in the non-fullerene PSCs with low bandgap *n*-OS **ITIC** as acceptor. The polymers of **J60** and **J61** with alkylthio substituents show red-shifted absorption, down-shifted HOMO energy levels, and better crystallinity in comparison with the polymer **J52** with alkyl substituent. Among the two alkylthio substituted polymers, **J61** with linear alkylthio substituent possesses stronger interchain interaction and shorter $\pi-\pi$ stacking distance in its polymer film and its blend films with **ITIC**. The PSCs based on **J61**/**ITIC** (1:1, w/w) with thermal annealing at 100 °C for 10 min exhibits a remarkably high PCE of 9.53% with a high J_{SC} of 17.43 mA/cm^2 and a V_{OC} of 0.89 V. The PCE of 9.53% is one of the highest photovoltaic efficiency in the non-fullerene PSCs reported so far in literature. Notably, the PCE and the IPCE_{max} of the **J61**/**ITIC**-based PSC are the highest values among the PSCs with E_{loss} less than 0.7 eV. The results highlighted that the side chain engineering is an effective way in tuning the electronic energy levels and interchain interaction of the polymer donor for matching with the *n*-OS acceptor in order to realize both high V_{OC} and high J_{SC} so that to get high PCE of the PSCs.

ASSOCIATED CONTENT

Supporting Information

The Supporting Information is available free of charge on the ACS Publications website at DOI: 10.1021/jacs.6b01744.

Experimental section, absorption spectra of the polymer/ITIC blend films, TGA plots, GIWAXS images of the pure ITIC film and the as-cast polymer/ITIC blend films, AFM height images of the blend films (PDF)

AUTHOR INFORMATION

Corresponding Authors

*zgzhangwhu@iccas.ac.cn
*liyf@iccas.ac.cn

Notes

The authors declare no competing financial interest.

ACKNOWLEDGMENTS

This work was supported by the Ministry of Science and Technology of China (973 Project, No. 2014CB643501) and NSFC (Nos. 91433117, 91333204, and 21374124) and the Strategic Priority Research Program of the Chinese Academy of Sciences (Grant No. XDB12030200).

REFERENCES

(1) Yu, G.; Gao, J.; Hummelen, J. C.; Wudl, F.; Heeger, A. J. *Science* **1995**, *270*, 1789.
(2) (a) Thompson, B. C.; Fréchet, J. M. J. *Angew. Chem., Int. Ed.* **2008**, *47*, 58. (b) Li, G.; Zhu, R.; Yang, Y. *Nat. Photonics* **2012**, *6*, 153. (c) Huang, Y.; Kramer, E. J.; Heeger, A. J.; Bazan, G. C. *Chem. Rev.* **2014**, *114*, 7006. (d) Cheng, Y.-J.; Yang, S.-H.; Hsu, C.-S. *Chem. Rev.* **2009**, *109*, 5868. (e) Li, C.; Liu, M.; Pschirer, N. G.; Baumgarten, M.; Müllen, K. *Chem. Rev.* **2010**, *110*, 6817.
(3) Liu, Y.; Zhao, J.; Li, Z.; Mu, C.; Ma, W.; Hu, H.; Jiang, K.; Lin, H.; Ade, H.; Yan, H. *Nat. Commun.* **2014**, *5*, 5293.
(4) Zhang, S.; Ye, L.; Zhao, W.; Yang, B.; Wang, Q.; Hou, J. *Sci. China: Chem.* **2015**, *58*, 248.
(5) Liao, S. H.; Jhuo, H. J.; Yeh, P. N.; Cheng, Y. S.; Li, Y. L.; Lee, Y. H.; Sharma, S.; Chen, S. A. *Sci. Rep.* **2014**, *4*, 6813.
(6) He, Z.; Xiao, B.; Liu, F.; Wu, H.; Yang, Y.; Xiao, S.; Wang, C.; Russell, T. P.; Cao, Y. *Nat. Photonics* **2015**, *9*, 174.
(7) Tumbleston, J. R.; Collins, B. A.; Yang, L.; Stuart, A. C.; Gann, E.; Ma, W.; You, W.; Ade, H. *Nat. Photonics* **2014**, *8*, 385.
(8) (a) Nielsen, C. B.; Holliday, S.; Chen, H.-Y.; Cryer, S. J.; McCulloch, I. *Acc. Chem. Res.* **2015**, *48*, 2803. (b) Lin, Y.; Zhan, X. *Acc. Chem. Res.* **2016**, *49*, 175. (c) Kim, T.; Kim, J.-H.; Kang, T. E.; Lee, C.; Kang, H.; Shin, M.; Wang, C.; Ma, B.; Jeong, U.; Kim, T.-S.; Kim, B. J. *Nat. Commun.* **2015**, *6*, 8547.

DOI: 10.1021/jacs.6b01744
J. Am. Chem. Soc. 2016, 138, 4657−4664

(9) Winzenberg, K. N.; Kemppinen, P.; Scholes, F. H.; Collis, G. E.; Shu, Y.; Singh, T. B.; Bilic, A.; Forsyth, C. M.; Watkins, S. E. *Chem. Commun.* **2013**, *49*, 6307.
(10) (a) Holliday, S.; Ashraf, R. S.; Nielsen, C. B.; Kirkus, M.; Röhr, J. A.; Tan, C.-H.; Collado-Fregoso, E.; Knall, A.-C.; Durrant, J. R.; Nelson, J.; McCulloch, I. *J. Am. Chem. Soc.* **2015**, *137*, 898. (b) Bloking, J. T.; Han, X.; Higgs, A. T.; Kastrop, J. P.; Pandey, L.; Norton, J. E.; Risko, C.; Chen, C. E.; Bredas, J.-L.; McGehee, M. D.; Sellinger, A. *Chem. Mater.* **2011**, *23*, 5484.
(11) (a) Li, S.; Liu, W.; Shi, M.; Mai, J.; Lau, T.-K.; Wan, J.; Lu, X.; Li, C.-Z.; Chen, H. *Energy Environ. Sci.* **2016**, *9*, 604. (b) Jung, J. W.; Jo, W. H. *Chem. Mater.* **2015**, *27*, 6038.
(12) Zhang, X.; Lu, Z.; Ye, L.; Zhan, C.; Hou, J.; Zhang, S.; Jiang, B.; Zhao, Y.; Huang, J.; Zhang, S.; Liu, Y.; Shi, Q.; Liu, Y.; Yao, J. *Adv. Mater.* **2013**, *25*, 5791.
(13) Kwon, O. K.; Uddin, M. A.; Park, J.-H.; Park, S. K.; Nguyen, T. L.; Woo, H. Y.; Park, S. Y. *Adv. Mater.* **2016**, *28*, 910.
(14) Li, H.; Earmme, T.; Ren, G.; Saeki, A.; Yoshikawa, S.; Murari, N. M.; Subramaniyan, S.; Crane, M. J.; Seki, S.; Jenekhe, S. A. *J. Am. Chem. Soc.* **2014**, *136*, 14589.
(15) Li, H.; Hwang, Y.-J.; Courtright, B. A. E.; Eberle, F. N.; Subramaniyan, S.; Jenekhe, S. A. *Adv. Mater.* **2015**, *27*, 3266.
(16) Lee, J.; Singh, R.; Sin, D. H.; Kim, H. G.; Song, K. C.; Cho, K. *Adv. Mater.* **2016**, *28*, 69.
(17) Zhong, H.; Wu, C.-H.; Li, C.-Z.; Carpenter, J.; Chueh, C.-C.; Chen, J.-Y.; Ade, H.; Jen, A. K. Y. *Adv. Mater.* **2016**, *28*, 951.
(18) Kang, S. J.; Ahn, S.; Kim, J. B.; Schenck, C.; Hiszpanski, A. M.; Oh, S.; Schiros, T.; Loo, Y.-L.; Nuckolls, C. *J. Am. Chem. Soc.* **2013**, *135*, 2207.
(19) Hartnett, P. E.; Timalsina, A.; Matte, H. S. S. R.; Zhou, N.; Guo, X.; Zhao, W.; Facchetti, A.; Chang, R. P. H.; Hersam, M. C.; Wasielewski, M. R.; Marks, T. J. *J. Am. Chem. Soc.* **2014**, *136*, 16345.
(20) Liu, Y.; Zhang, L.; Lee, H.; Wang, H.-W.; Santala, A.; Liu, F.; Diao, Y.; Briseno, A. L.; Russell, T. P. *Adv. Energy Mater.* **2015**, *5*, 1500195.
(21) Shivanna, R.; Shoaee, S.; Dimitrov, S.; Kandappa, S. K.; Rajaram, S.; Durrant, J. R.; Narayan, K. S. *Energy Environ. Sci.* **2014**, *7*, 435.
(22) Sharenko, A.; Proctor, C. M.; van der Poll, T. S.; Henson, Z. B.; Nguyen, T.-Q.; Bazan, G. C. *Adv. Mater.* **2013**, *25*, 4403.
(23) Zhao, J.; Li, Y.; Lin, H.; Liu, Y.; Jiang, K.; Mu, C.; Ma, T.; Lai, J. Y. L.; Hu, H.; Yu, D.; Yan, H. *Energy Environ. Sci.* **2015**, *8*, 520.
(24) (a) Zang, Y.; Li, C.-Z.; Chueh, C.-C.; Williams, S. T.; Jiang, W.; Wang, Z.-H.; Yu, J.-S.; Jen, A. K. Y. *Adv. Mater.* **2014**, *26*, 5708. (b) Lin, H.; Chen, S.; Li, Z.; Lai, J. Y. L.; Yang, G.; McAfee, T.; Jiang, K.; Li, Y.; Liu, Y.; Hu, H.; Zhao, J.; Ma, W.; Ade, H.; Yan, H. *Adv. Mater.* **2015**, *27*, 7299.
(25) Zhong, Y.; Trinh, M. T.; Chen, R.; Purdum, G. E.; Khlyabich, P. P.; Sezen, M.; Oh, S.; Zhu, H.; Fowler, B.; Zhang, B.; Wang, W.; Nam, C.-Y.; Sfeir, M. Y.; Black, C. T.; Steigerwald, M. L.; Loo, Y.-L.; Ng, F.; Zhu, X. Y.; Nuckolls, C. *Nat. Commun.* **2015**, *6*, 8242.
(26) Hwang, Y.-J.; Li, H.; Courtright, B. A. E.; Subramaniyan, S.; Jenekhe, S. A. *Adv. Mater.* **2016**, *28*, 124.
(27) Meng, D.; Sun, D.; Zhong, C.; Liu, T.; Fan, B.; Huo, L.; Li, Y.; Jiang, W.; Choi, H.; Kim, T.; Kim, J. Y.; Sun, Y.; Wang, Z.; Heeger, A. J. *J. Am. Chem. Soc.* **2016**, *138*, 375.
(28) Gao, L.; Zhang, Z.-G.; Xue, L.; Min, J.; Zhang, J.; Wei, Z.; Li, Y. *Adv. Mater.* **2016**, *28*, 1884.
(29) Lin, Y.; Wang, J.; Zhang, Z.-G.; Bai, H.; Li, Y.; Zhu, D.; Zhan, X. *Adv. Mater.* **2015**, *27*, 1170.
(30) (a) Zhan, X.; Tan, Z. a.; Domercq, B.; An, Z.; Zhang, X.; Barlow, S.; Li, Y.; Zhu, D.; Kippelen, B.; Marder, S. R. *J. Am. Chem. Soc.* **2007**, *129*, 7246. (b) Zhou, E.; Cong, J.; Wei, Q.; Tajima, K.; Yang, C.; Hashimoto, K. *Angew. Chem., Int. Ed.* **2011**, *50*, 2799. (c) Ye, L.; Jiao, X.; Zhou, M.; Zhang, S.; Yao, H.; Zhao, W.; Xia, A.; Ade, H.; Hou, J. *Adv. Mater.* **2015**, *27*, 6046. (d) Zhang, Z.-G.; Li, Y. *Sci. China: Chem.* **2015**, *58*, 192.
(31) (a) Cui, C.; Wong, W.-Y.; Li, Y. *Energy Environ. Sci.* **2014**, *7*, 2276. (b) Ye, L.; Zhang, S.; Zhao, W.; Yao, H.; Hou, J. *Chem. Mater.* **2014**, *26*, 3603. (c) Cui, C.; He, Z.; Wu, Y.; Cheng, X.; Wu, H.; Li, Y.; Cao, Y.; Wong, W.-Y. *Energy Environ. Sci.* **2016**, *9*, 885.
(32) (a) Cabanetos, C.; El Labban, A.; Bartelt, J. A.; Douglas, J. D.; Mateker, W. R.; Fréchet, J. M. J.; McGehee, M. D.; Beaujuge, P. M. *J. Am. Chem. Soc.* **2013**, *135*, 4656. (b) Chen, M. S.; Lee, O. P.; Niskala, J. R.; Yiu, A. T.; Tassone, C. J.; Schmidt, K.; Beaujuge, P. M.; Onishi, S. S.; Toney, M. F.; Zettl, A.; Fréchet, J. M. J. *J. Am. Chem. Soc.* **2013**, *135*, 19229.
(33) Min, J.; Zhang, Z.-G.; Zhang, S.; Li, Y. *Chem. Mater.* **2012**, *24*, 3247.
(34) (a) Price, S. C.; Stuart, A. C.; Yang, L.; Zhou, H.; You, W. *J. Am. Chem. Soc.* **2011**, *133*, 4625. (b) Li, W.; Albrecht, S.; Yang, L.; Roland, S.; Tumbleston, J. R.; McAfee, T.; Yan, L.; Kelly, M. A.; Ade, H.; Neher, D.; You, W. *J. Am. Chem. Soc.* **2014**, *136*, 15566.
(35) Carsten, B.; He, F.; Son, H. J.; Xu, T.; Yu, L. *Chem. Rev.* **2011**, *111*, 1493.
(36) Zhang, Z.-G.; Qi, B.; Jin, Z.; Chi, D.; Qi, Z.; Li, Y. F.; Wang, J. Z. *Energy Environ. Sci.* **2014**, *7*, 1966.
(37) Rivnay, J.; Mannsfeld, S. C. B.; Miller, C. E.; Salleo, A.; Toney, M. F. *Chem. Rev.* **2012**, *112*, 5488.
(38) (a) Veldman, D.; Meskers, S. C. J.; Janssen, R. A. J. *Adv. Funct. Mater.* **2009**, *19*, 1939. (b) Faist, M. A.; Kirchartz, T.; Gong, W.; Ashraf, R. S.; McCulloch, I.; de Mello, J. C.; Ekins-Daukes, N. J.; Bradley, D. D. C.; Nelson, J. *J. Am. Chem. Soc.* **2012**, *134*, 685. (c) Kawashima, K.; Tamai, Y.; Ohkita, H.; Osaka, I.; Takimiya, K. *Nat. Commun.* **2015**, *6*, 10085.

DOI: 10.1021/jacs.6b01744
J. Am. Chem. Soc. 2016, 138, 4657−4664